

# Biosensors for Efficient Diagnosis of Leishmaniasis: Innovations in Bioanalytics for a Neglected Disease

Ângelo C. Perinoto,<sup>†</sup> Rafael M. Maki,<sup>‡</sup> Marcelle C. Colhone,<sup>§</sup> Fabiana R. Santos,<sup>§</sup> Vanessa Migliaccio,<sup>§</sup> Katia R. Daghestanli,<sup>||</sup> Rodrigo G. Stabeli,<sup>⊥</sup> Pietro Ciancaglini,<sup>§</sup> Fernando V. Paulovich,<sup>‡</sup> Maria C. F. de Oliveira,<sup>‡</sup> Osvaldo N. Oliveira, Jr.,<sup>†</sup> and Valtencir Zucolotto\*<sup>†</sup>

Instituto de Física de São Carlos, USP, CP 369, 13560-970 São Carlos, SP, Brazil, Instituto de Ciências Matemáticas e de Computação, USP, CP 668, 13560-970 São Carlos, SP, Brazil, Faculdade de Filosofia, Ciências e Letras de Ribeirão Preto, USP, Ribeirão Preto, SP, Brazil, Departamento de Biofísica da Escola Paulista de Medicina, UNIFESP, São Paulo, SP, Brazil, and Universidade Federal de Rondônia (UNIR) and Fundação Oswaldo Cruz - Fiocruz Noroeste, Rondônia, Brazil

The need for reliable, fast diagnostics is closely linked to the need for safe, effective treatment of the so-called “neglected” diseases. The list of diseases with no field-adapted diagnostic tools includes leishmaniasis, shigella, typhoid, and bacterial meningitis. Leishmaniasis, in particular, is a parasitic disease caused by *Leishmania* spp. transmitted by infected phlebotomine sandfly, which remains a public health concern in developing countries with ca. 12 million people infected and 350 million at risk of infection. Despite several attempts, methods for diagnosis are still noneffective, especially with regard to specificity due to false positives with Chagas’ disease caused by *Trypanosoma cruzi*. Accepted golden standards for detecting leishmaniasis involve isolation of parasites either microscopically, or by culture, and in both methods specimens are obtained by invasive means. Here, we show that efficient distinction between cutaneous leishmaniasis and Chagas’ disease can be obtained with a low-cost biosensor system made with nanostructured films containing specific *Leishmania amazonensis* and *T. cruzi* antigens and employing impedance spectroscopy as the detection method. This unprecedented selectivity was afforded by antigen–antibody molecular recognition processes inherent in the detection with the immobilized antigens, and by statistically correlating the electrical impedance data, which allowed distinction between real samples that tested positive for Chagas’ disease and leishmaniasis. Distinction could be made of blood serum samples containing  $10^{-5}$  mg/mL of the antibody solution in a few minutes. The methods used here are generic and can be extended to any type of biosensor, which is important for an effective diagnosis of many other diseases.

Leishmaniasis is a parasitic neglected disease that remains as a major public health concern, especially for its high incidence in developing countries. It affects around 12 million people, and 350 million are at risk of infection.<sup>1</sup> The disease is caused by *Leishmania* spp., transmitted by infected phlebotomine sandfly. Depending on the type of parasite causing the infection, leishmaniasis may be classified as visceral leishmaniasis (VL), diffuse cutaneous leishmaniasis, mucocutaneous leishmaniasis, and cutaneous leishmaniasis (CL).<sup>2,3</sup> Many research groups have focused on novel strategies for treatment and for low-cost, effective diagnosis systems.<sup>4,5</sup> Despite such efforts, diagnosis methods are still noneffective, with limitations regarding cost, sensitivity, difficulty in using under field conditions, and specificity.<sup>6</sup> The latter limitation, in particular, applies to cases of cross-reaction with Chagas’ disease,<sup>7,8</sup> and to a lesser extent to tuberculosis and leprosy.<sup>5</sup> Cutaneous leishmaniasis (CL) is frequently diagnosed by classic clinical investigation, or via laboratorial diagnosis under microscopic examination of smears or biopsies of skin lesions.<sup>9,10</sup> Culturing of replicative *Leishmania* specimens from the skin lesion border may also be performed.<sup>4,10,11</sup> These methods, however, often lead to misdiagnosis; the culture assays are positive in only ca. 70% when the patient has a severe disease.<sup>11</sup> Moreover, contaminations may affect culture procedures, whereas the his-

\* To whom correspondence should be addressed. E-mail: zuco@if.sc.usp.br.

<sup>†</sup> Instituto de Física de São Carlos.

<sup>‡</sup> Instituto de Ciências Matemáticas e de Computação.

<sup>§</sup> Faculdade de Filosofia, Ciências e Letras de Ribeirão Preto.

<sup>||</sup> Departamento de Biofísica da Escola Paulista de Medicina.

<sup>⊥</sup> Universidade Federal de Rondonia and Fundação Oswaldo Cruz.

- (1) Usdin, M.; Guillerm, M.; Chirac, P. *Nature* **2006**, *441*, 283–284.
- (2) Desjeux, P. *Nat. Rev. Microbiol.* **2004**, *2*, 692–693.
- (3) Calderon, L. A.; Silva-Jardim, I.; Zuliani, J. P.; Silva, A. A.; Ciancaglini, P.; da Silva, L. H. P.; Stabeli, R. G. *J. Braz. Chem. Soc.* **2009**, *20*, 1011–1023.
- (4) Vega-López, F. *Curr. Opin. Infect. Dis.* **2003**, *16*, 97–101.
- (5) Singh, S.; Sivakumar, R. *J. Postgrad. Med. (Bombay)* **2003**, *49*, 55–60.
- (6) Romero, H. D.; Silva, L. A.; Silva-Vergara, M. L.; Rodriguez, V.; Costa, R. T.; Guimarães, S. F.; Alecrim, W.; Moraes-Souza, H.; Prata, A. *Am. J. Trop. Med. Hyg.* **2009**, *81*, 27–33.
- (7) Nour, N. B.; Gianinazzi, C.; Gorcii, M.; Müller, N.; Nouri, A.; Babba, H.; Gottstein, B. *Trans. R. Soc. Trop. Med. Hyg.* **2009**, *103*, 355–364.
- (8) Castro, E. A.; Thomaz-Socol, V.; Augur, C.; Luz, E. *Exp. Parasitol.* **2007**, *117*, 13–21.
- (9) Boggild, A. K.; Valencia, B. M.; Espinosa, D.; Veland, N.; Ramos, A. P.; Arevalo, J.; Llanos-Cuentas, A.; Low, D. E. *Clin. Infect. Dis.* **2010**, *50*, 1–6.
- (10) Herwaldt, B. L. *Lancet* **1999**, *354*, 1191–1199.
- (11) Weigle, K. A.; Labrada, L. A.; Lozano, C.; Santrich, C.; Barker, D. C. *J. Clin. Microbiol.* **2002**, *40*, 601–606.

topathological examination is often difficult due to dehydration and deformation of amastigotes.<sup>2,4</sup> All of these procedures are expensive and time-consuming, causing delay in the diagnosis and hindering precocious treatment of the patient.

The low sensitivity and time-consuming limitations exhibited by cell culture and microscopic examination of skin lesions may be overcome by using immunodetection assays, in which antigens are applied for direct detection of specific antileishmania antibodies. Diagnosis of visceral leishmaniasis has been performed in immunoblotting assays with *Leishmania* antigens.<sup>12</sup> However, such methods are limited in the case of cutaneous leishmaniasis, for anti-*Leishmania* antibodies are present in the serum at very low levels.<sup>5</sup> Molecular analyses have also been applied to detect DNA and RNA from leishmania parasites, with PCR methods being by far the most used.<sup>13,14</sup> Despite the high sensitivity and specificity of the PCR methodology, through which specific sequences of the parasites can be determined, the method is not cost-effective, being unsuitable for field diagnosis.

The limitations found in immunoassays and molecular diagnosis have motivated the development of integrated electronic biosensors systems, which in most cases employ nanostructured biomaterials. These systems are capable of detecting analytes via specific recognition based upon interaction between protein and ligands or antigens and antibodies.<sup>15,16</sup> Integrated biosensors may exhibit high sensitivity and specificity, as exemplified with the detection of pasteurellosis.<sup>16</sup> Detection is performed via electrical measurements, following the concept of a taste sensor, in which the bioreceptor material is immobilized on the gaps of an interdigitated electrode and immersed in aqueous solutions containing different concentrations of the analyte.<sup>16</sup> Differences in the electrical capacitance of the electrodes are correlated to the type and concentration of the analytes using equivalent electric circuits. These circuits represent the experimental system, that is, metallic tracks covered with a layer of biological bioreceptors, immersed in an electrolyte.<sup>17</sup> The latter biodetection systems are user-friendly and are capable of providing in-field diagnosis within a short period of time. These technical characteristics are advantageous for the high throughput inherent in new drug and diagnosis tests.

In this Article, we present a nanostructured biosensor system to detect specific anti-leishmania antibodies using capacitance measurements as the detection method. The system is comprised of phospholipid liposomes<sup>18</sup> incorporating membrane antigenic proteins as the immobilized phase, which had been anchored to the surface of interdigitated electrodes. The electrodes containing antigenic proteins were used to detect antibodies, in which the biological reaction was converted into variations in the electrical

response (capacitance). Here, we selected a pool of membrane antigenic proteins from *L. amazonensis* because of the high incidence of this species in the north region of Brazil. However, the system described here may be applied to any other *Leishmania* species.

The proteoliposomes incorporating the antigenic proteins were prepared according to a well-established methodology,<sup>18</sup> which is described in the Experimental Section. The freshly prepared proteoliposomes were immobilized on interdigitated electrodes using the layer-by-layer technique,<sup>19,20</sup> in conjunction with polyamidoamine dendrimers generation 4 (PAMAM). Because of their branched, porous structure, dendrimers have been used for immobilizing proteins in biosensors, with enhanced sensitivity and short response times due to diffusion of analytes through the multilayer structure.<sup>21</sup> Furthermore, the porous architecture of the film is crucial for confining electrical charges within its structure (e.g., charges generated in the biological reaction), which are responsible for the detectable changes in the electrical response.<sup>21</sup>

## EXPERIMENTAL SECTION

**Materials.** All solutions were prepared using Millipore (Bedford, MA) DirectQ ultrapure water. Tris(hydroxymethyl)amino-methane (TRIS), bovine serum albumine (BSA), Schneider's insect medium, ethylenediaminetetraacetic (EDTA), phenylmethylsulfonyl fluoride (PMSF), trans-epoxysuccinyl-L-leucinamido-(4-guani-dino)butane (E-64), 1,10-phenanthroline dipalmitoylphosphatidylcholine (DPPC), dipalmitoylphosphatidylserine (DPPS), cholesterol, and sodium dodecyl sulfate (SDS) were purchased from Sigma (St. Louis, MO); calbisorb resin was from Calbiochem (San Diego, CA). Polyamidoamine generation 4 dendrimer (PAMAM) and poly(allylamine hydrochloride) (PAH) (used as polycations) and poly(vinyl) sulfonic acid (PVS) (polyanion) were purchased from Aldrich and used without further purification. Gold (Au) interdigitated electrodes were lithographically fabricated at the National Synchrotron Laboratory facilities, Campinas, Brazil. Au tracks (10  $\mu\text{m}$  wide  $\times$  70 nm thick) were deposited onto BK7 glass substrates with a separation distance of 10  $\mu\text{m}$  among the tracks.

**Parasites.** The parasite strain IFLA/BR/67/PH8 of *Leishmania amazonensis* was maintained in BALB/c mice (Nunes et al., 1997; Noronha et al., 1998; Santos et al., 2006).

**Serum Preparation of *L. amazonensis* and *T. cruzi*.** Blood samples were collected from the BALB/c mice naïve, mice infected subcutaneously in the hind footpad with  $10^6$  stationary growth phase *L. amazonensis* promastigotes, and mice infected intraperitoneally with a nonlethal dose of 300 blood-form trypomastigotes of the Y strain of *T. cruzi*. The serum against total *L. amazonensis* and *T. cruzi* antigenic determinants was obtained from coagulated blood by centrifugation and frozen at  $-20$  °C until use. The total IgG of positive and negative serum samples was purified with the Protein G Sepharose 4 Fast Flow (GE Healthcare).

- (12) Santos-Gomes, G.; Gomes-Pereira, S.; Campino, Araújo, L. M. A.; Abranches, P. *J. Clin. Microbiol.* **2000**, *38*, 175–178.
- (13) Romero, G. A. S.; Noronha, E. F.; Pirmez, C.; Pires, F. E. S. S.; Fernandes, O.; Nehme, N. S.; Cupolillo, E.; Firoozmand, L.; da Graça, G. C.; Volpini, A.; Santos, S. L.; Romanha, A. J. *Acta Trop.* **2009**, *109*, 74–77.
- (14) Reithinger, R.; Dujardin, J.-C. *J. Clin. Microbiol.* **2007**, *45*, 21–25.
- (15) Zucolotto, V.; Pinto, A. P. A.; Tumolo, T.; Moraes, M. L.; Baptista, M. S.; Riul, A., Jr.; Araújo, A. P. U.; Oliveira, O. N., Jr. *Biosens. Bioelectron.* **2006**, *21*, 1320–1326.
- (16) Zucolotto, V.; Daghasanli, K. R. P.; Hayasaka, C. O.; Riul, A., Jr.; Ciancaglini, P.; Oliveira, O. N., Jr. *Anal. Chem.* **2007**, *79*, 2163–2167.
- (17) Taylor, D. M.; MacDonald, A. G. *J. Phys. D: Appl. Phys.* **1987**, *20*, 1277–1283.
- (18) Santos, F. R.; Ferraz, D. B.; Daghasanli, K. R. P.; Ramalho-Pinto, F. J.; Ciancaglini, P. *J. Membr. Biol.* **2006**, *210*, 173–181.

- (19) Mattoso, L. H. C.; Zucolotto, V.; Patterno, L. G.; Van Griethuijsen, R.; Ferreira, M.; Campana, S. P.; Oliveira, O. N., Jr. *Synth. Met.* **1995**, *71*, 2037–2038.
- (20) Decher, G. *Science* **1997**, *277*, 1232–1237.
- (21) Fernandes, E. G. R.; Vieira, N. C. S.; de Queiroz, A. A. A.; Guimarães, F. E. G.; Zucolotto, V. *J. Phys. Chem. C* **2010**, *114*, 6478–6483.

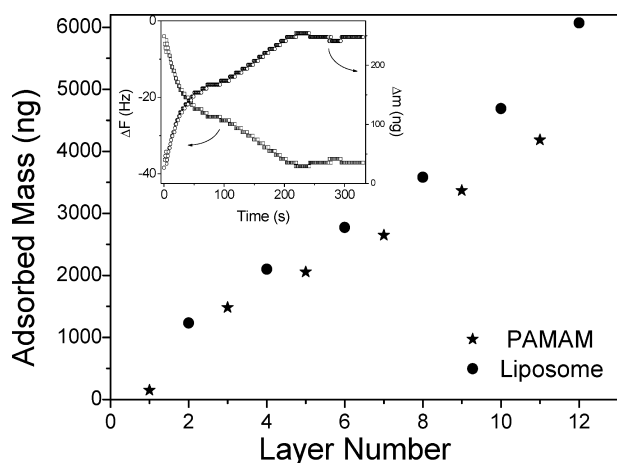


**Figure 1.** Amount of PAMAM and proteoliposome adsorbed at each deposition step. Inset: Frequency change and adsorbed mass for PAMAM first layer as a function of deposition time, as measured with a QCM.

**Solubilization of *L. amazonensis* Membrane Proteins and Proteoliposomes Preparation.** The procedures to obtain the crude extract and dissolve the membrane protein of *L. amazonensis* were performed as described in Santos et al.<sup>18</sup> Briefly, the frozen pellets of amastigotes were resuspended in 5 mM TRIS-HCl buffer, pH 7.5, containing a protease inhibitor cocktail (1 mM EDTA, 1.6 mM PMSF, 0.1 mM E-64, and 1 mM 1,10-phenanthroline). The suspension was sonicated at 4 °C with three 30 s blasts at 60 W. SDS was added to a sample with 0.5 mg/mL in protein

of this crude extract of the parasite to reach 0.1% (w/v) at 4 °C. The solubilization of the crude extract was carried out instantaneously, followed by separation with ultracentrifugation at 100 000g for 1 h. The solubilized protein concentration was estimated in the supernatant, in the presence of SDS 2.0% (w/v), using crystallized BSA as standard. Proteoliposomes were prepared by the cosolubilization method, using a DPPC:DPPS:cholesterol ratio of 5:1:4 (w/w) as described elsewhere.<sup>22</sup>

**Electrode Preparation.** PAMAM and proteoliposomes were used at 1 and 0.7 mg/mL, respectively, in a 5 mM Tris-HCl pH 7.5 buffer solution. Nanostructured LbL films containing up to 12 PAMAM/proteoliposome bilayers were assembled on quartz slides for UV-vis measurements, and 5-bilayer PAMAM/proteoliposome films were deposited onto gold interdigitated electrodes for capacitance measurements. All substrates were previously cleaned in a  $\text{NH}_4\text{OH}/\text{H}_2\text{O}_2/\text{H}_2\text{O}$  (5:1:1 v/v) bath for 20 min. Deposition of the multilayers was carried out by immersing the quartz slides or interdigitated electrodes alternately into the PAMAM (polycationic) and proteoliposomes (polyanionic) solutions for 5 and 15 min, respectively. After deposition of each layer, the substrate/film system was immersed for 1 min in the buffer solution. The deposition process was monitored at each deposited layer using a quartz crystal microbalance (QCM).

**Electrical Detection of Antiserum.** Capacitance measurements were performed with a Solartron impedance/gain phase analyzer (model 1260A). Unlike the electrochemical experiments, the in-plane capacitance of the film deposited between the tracks

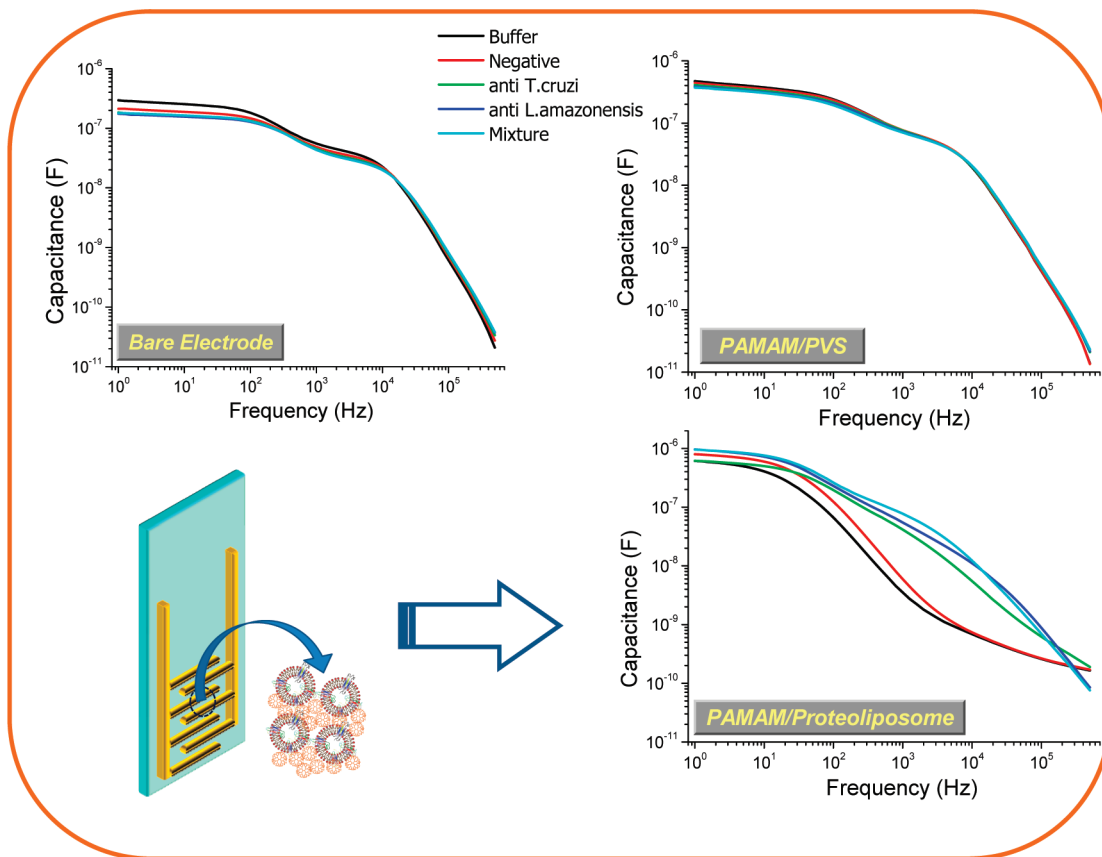


**Figure 2.** Capacitance versus frequency curves for three electrodes immersed into 10<sup>-5</sup> mg/mL antibody solutions, as indicated in the legend. The electrodes comprised a bare electrode (upper left), an electrode containing 5 bilayers of PAMAM/PVS (upper right), and the electrode containing 5 bilayers of PAMAM/proteoliposome (lower right).



of the interdigitated electrode was collected in a frequency range from 10 Hz to 1 MHz, with no need of a reference electrode. All measurements were taken with the films deposited onto gold interdigitated electrodes immersed in buffer, and in positive IgG antibody solutions at different concentrations from  $10^{-2}$  to  $10^{-10}$  mg/mL. The negative IgG solutions were comprised of purified IgGs anti-*T. cruzi* and were employed at the same concentration range. Capacitance curves were taken three times for each sensor, after soaking for 20 min in the analytical solutions. After each measurement, the sensors were rinsed in the buffer solution. For comparison, the same sets of experiments were carried out using bare interdigitated electrodes and interdigitated electrodes coated with a 5-bilayer PAMAM/PVS film (in the absence of proteoliposomes).

## RESULTS AND DISCUSSION

The immobilization process occurred via the alternate immersion of interdigitated electrodes into the PAMAM or proteoliposome buffer solutions, with adsorption taking place spontaneously within 5 min for PAMAM and ca. 15 min for the proteoliposomes. The adsorption process is depicted in Figure 1, in which the alternate adsorption of PAMAM (cationic) and the proteoliposome (anionic) layers was followed by QCM. Adsorption is quite efficient, with deposition of ca. 500 ng of proteoliposome in each deposition step, while for the PAMAM layer the deposited mass was ca. 200 ng. The electrodes containing the PAMAM/proteoliposome LbL film were used to detect and distinguish between *L. amazonensis* and *T. cruzi* purified antibodies (purified IgGs) via impedance measurements. The electrodes were immersed in different antibodies solutions at several concentrations, and the changes in the capacitance of the electrodes, under an applied AC signal, were recorded as a function of frequency, as reported for capacitance biosensors.<sup>15,16</sup> Purified anti-*L. amazonensis*, *T. cruzi*, and negative (mouse serum in the absence of antibodies against parasites) antibodies solutions were employed at concentrations ranging from  $10^{-1}$  to  $10^{-10}$  mg/mL. For comparison, measurements were also taken in a buffer solution, containing no antibodies, as the control, in a mixture of anti-*L. amazonensis* and anti-*T. cruzi*, and negative antibody solutions.

As a proof-of-concept, the ability of the electrode bearing the proteoliposomes to distinguish among different antibodies is shown in Figure 2, which also brings the response of a bare electrode and of an electrode containing PAMAM adsorbed in conjunction with poly(vinyl sulfonic acid) (PVS). The latter electrode was used to verify the ability of an electrode containing an organic film (where no specific interactions are expected) to detect the specific antibodies. There is little change in capacitance for the bare electrode and the PAMAM/PVS electrode upon immersing into the solutions with  $10^{-5}$  mg/mL antibodies. In contrast, the capacitance curve changed significantly for the PAMAM/proteoliposome electrode, especially in the frequency region from  $10^2$  to  $10^5$  Hz. Of special interest is the frequency region between 1 and 10 kHz, for which the selectivity of the PAMAM/proteoliposome electrode was highest. The capacitance for the mixture of antibodies was practically the same as that for the positive anti-*L. amazonensis* IgGs (at 10 kHz), which reveals that specific interactions occur upon immersion of the electrode in the mixture of IgGs, with only the positive anti-*L. amazonensis* antibodies binding to the electrode. This

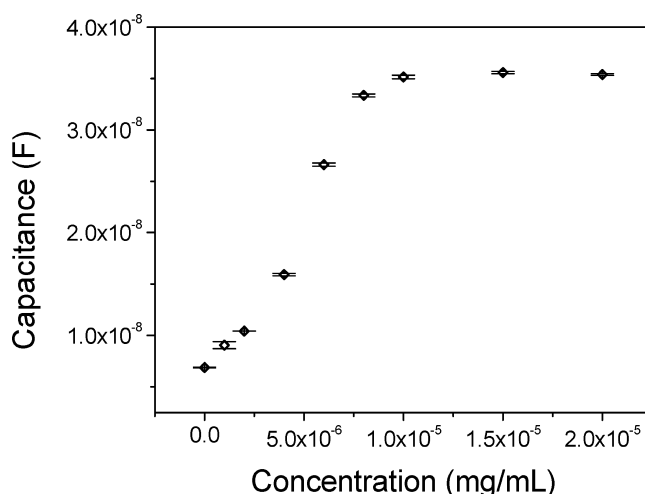


**Figure 3.** Analytical curve showing the dependence of the capacitance on the amount of specific anti-*L. amazonensis* IgG in the solution. The electrode contained 5 PAMAM/proteoliposomes bilayers.

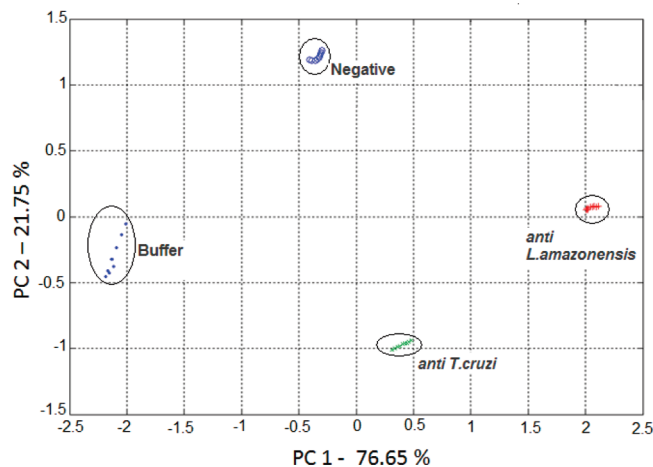


**Figure 4.** PCA plot obtained upon using capacitance data from the three electrodes at a frequency of 100 Hz. The capacitance values were collected with the electrodes immersed in the solutions containing buffer (Tris 5 mM) (●) and different antibodies at  $10^{-5}$  mg/mL: negative (○), anti-*T. cruzi* (×), and positive anti-*L. amazonensis* (+).

selectivity also applies to the negative antibodies, for the capacitance of the electrode immersed in the buffer solution was the same as that of the electrodes immersed in the solution with negative antibodies (at 10 kHz). Furthermore, with the PAMAM/proteoliposome electrode, it is also possible to distinguish the capacitance signal of the anti-*T. cruzi* IgGs solution, which is separated from the other systems. The latter proves that the electrode is quite selective for anti-*L. amazonensis* IgGs, and no-cross reaction with *T. cruzi* occurs at this frequency region.

The dependence between the capacitance and the concentration of positive IgGs has been investigated to yield the analytical curve of Figure 3. The data clearly point to an almost linear increase in capacitance as a function of the IgGs concentration until a plateau is reached at ca.  $1 \times 10^{-5}$  mg/mL. At this concentration, all the sites in the immobilized layers available for binding the IgGs had probably been taken. From a physical point of view, the increase in

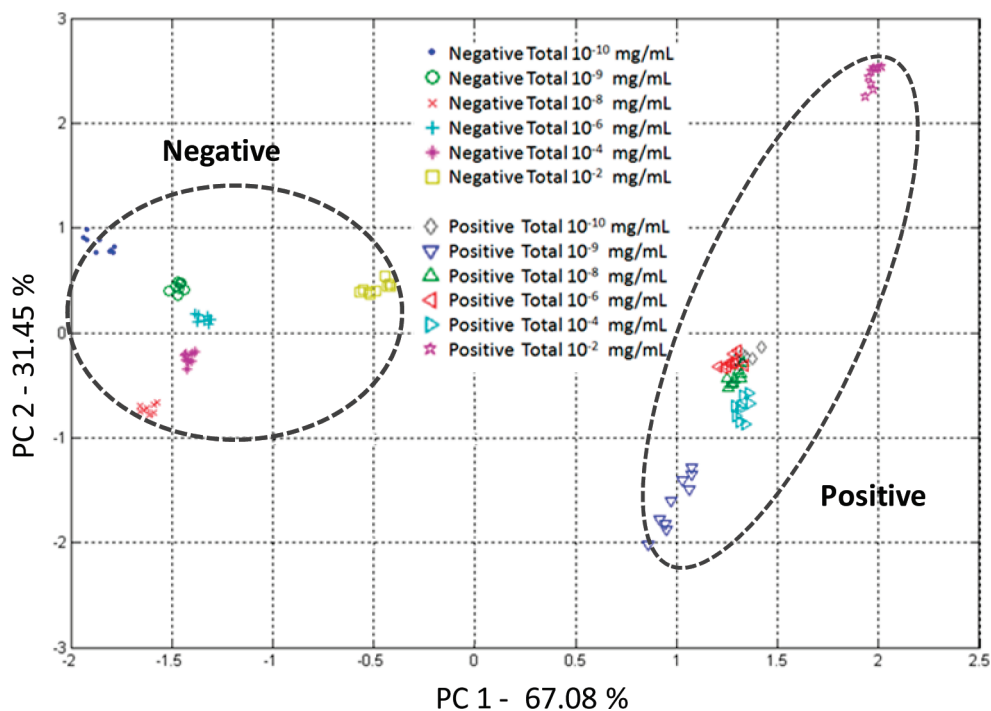


**Figure 5.** PCA plot built with capacitance data from the three electrodes immersed in total serum samples from mice infected with *L. amazonensis* (positive total serum) and from mice infected with *T. cruzi* (negative total serum). The total serum in both cases was diluted from  $10^{-2}$  to  $10^{-10}$  mg/mL.

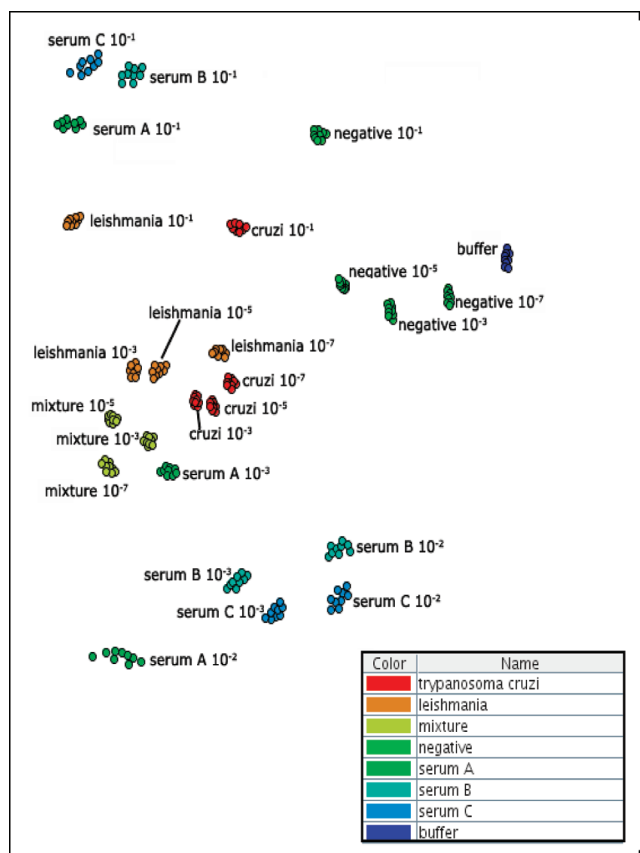


**Figure 6.** Sammon's mapping projection for all samples, with the standardization procedure applied to the  $m$ -dimensional data samples. In this case, analyses were performed using data from four sensors, including a sensor based on immobilized proteoliposomes containing *T. cruzi* antigens.

capacitance may be related to changes in the dielectric constant of the material, in this case, the PAMAM/proteoliposome film, deposited on the gaps of gold tracks in the interdigitated electrode. The increase in capacitance is probably related to the generation of additional interfaces in the dielectric region due to adsorption of antibodies.

To improve the distinguishing ability of the biosensing system, we combined the capacitance values at 1 kHz obtained with the three electrodes, (i) bare electrode, (ii) electrode containing 5 PAMAM/PVS bilayers, and (iii) electrode containing 5 PAMAM/proteoliposome bilayers, and analyzed using principal component analysis (PCA). The PCA plot in Figure 4 demonstrates that all analytes can be distinguished for a concentration of  $10^{-5}$  mg/mL of IgGs.

To reduce costs for sample preparation and IgGs purification, as required for in field diagnosis, we investigated the ability of the electrodes to detect specific antibodies in total serum samples from mice infected with *L. amazonensis*, and also from mice infected with *T. cruzi* (see details in the Experimental Section). The total serum had been diluted in buffer at concentrations from  $10^{-2}$  to  $10^{-10}$  mg/mL. Note that the positive serum concentration at  $10^{-10}$  mg/mL implies a much lower aliquot for positive anti-*L. amazonensis* IgGs. Surprisingly, the electrodes could still distinguish between the two total serum samples, as depicted in the PCA plot of Figure 5. The data from negative samples were located in the left part of the plot, whereas data from positive samples were located in the right side of the chart. The latter indicated the capacity of the methods to detect positive anti-*L. amazonensis* in the total serum, as well as the ability to distinguish the data from anti-*T. cruzi* IgGs. Therefore, no cross-reactions could be noted, and the performance of the diagnosis system is optimized.

We also stress that use can be made of multidimensional projection techniques as described elsewhere<sup>23</sup> to visualize the impedance data for all the samples tested in the same plot. Figure 6 shows that a complete separation is reached for the various samples when the Sammon's mapping method is employed. Further details of the application of projection techniques to this biosensing data can be found in ref 24.

## CONCLUSIONS

The need for cost-effective, reliable diagnosis methods, through which leishmaniasis can be identified and treated in the very early stages, is evidenced by the fact that first and second-line drugs used for treating it present high toxicity, several side effects, and require long-term management. In this Article, we showed a

- 
- (22) Daghestanli, K. R. P.; Ferreira, R. B.; Thedei, G., Jr.; Maggio, B.; Ciancaglini, P. *Colloids Surf., B* **2004**, *36*, 127–137.
- (23) Siqueira, J. R., Jr.; Maki, R. M.; Paulovich, F. V.; Werner, C. F.; Poghossian, A.; Oliveira, M. C. F.; Zucolotto, V.; Oliveira, O. N., Jr.; Schöning, M. J. *Anal. Chem.* **2010**, *82*, 61–65.
- (24) Paulovich, F. V.; Maki, R. M.; de Oliveira, M. C. F.; Colhone, M. C.; Santos, F. R.; Migliaccio, V.; Ciancaglini, P.; Daghestanli, K. R.; Stabeli, R. G.; Perinotto, A. C.; Oliveira, O. N., Jr.; Zucolotto, V. *Anal. Chem.*, submitted.

promising way for rapid, accurate diagnosis of *Leishmania* infections using interdigitated electrodes containing immobilized proteoliposomes. Electrical capacitance measurements allowed the detection of specific anti-*L. amazonensis* antibodies at concentrations down to  $10^{-5}$  mg/mL. The use of PCA to statistically correlate the capacitance data permitted the distinction between positive and negative total serum samples. The methods used here are generic and may be extended to the diagnosis of bacterial, protozoan, and helminth infectious diseases affecting developing countries, including tuberculosis, malaria, and other neglected diseases, such as the African sleeping sickness, onchocerciasis, lymphatic filariasis, and schistosomiasis.

## ACKNOWLEDGMENT

This work was supported by FAPESP, CNPq, and Capes (Brazil).

Received for review July 20, 2010. Accepted October 4, 2010.

AC101920T